Turkish Journal of Electrical Engineering & Computer Sciences

http://journals.tubitak.gov.tr/elektrik/

Research Article

Turk J Elec Eng & Comp Sci
(2016) 24: 4218 – 4230

doi:10.3906/elk-1502-166

Stability assessment of isolated six-phase induction generator feeding static loads

Kiran SINGH*, **Girish Kumar SINGH**
Department of Electrical Engineering, Indian Institute of Technology, Roorkee, Uttarakhand, India

Received: 19.02.2015 • **Accepted/Published Online:** 28.07.2015 • **Final Version:** 20.06.2016

Abstract: This paper presents the stability analysis of a six-phase self-excited induction generator (SP-SEIG) based on the eigenvalue stability criteria for its linearized model. This demonstrates the small signal stability behavior during steady-state operating conditions. The eigenvalue approach also establishes an opportunity to correlate eigenvalues with machine parameters. The investigation in this paper reveals that the eigenvalues are dependent upon the machine parameters, and the most critical parameter is the variation in magnetizing inductance (L_m). The eigenvalues are varied in accordance with the machine variables and give focus to the stabilization of the SP-SEIG. A particular voltage build-up phenomenon is also experimentally verified to validate the proposed analytical approach in this paper.

Key words: Modeling, six-phase, self-excited, induction generator, small-displacement, stability

1. Introduction

The stability of electrical machines is an important factor for consideration and is directly affected by many design parameters during steady-state operation. The first overall scenario on the stability of AC machines was developed in 1965 using the root locus technique [1]. The instability of the induction motor, which is fed by the frequency inverter, was analyzed in [2]. Other works [3–8] analyzed an induction motor drive with different schemes of rectifier-inverter, single cage, controlled current, current source inverter, double cage, and voltage source inverter, using Nyquist stability criterion, root-locus technique, transfer function technique, a linearized small signal model, decoupled boundary layer model, and Lyapunov's first method, respectively. All these works only analyzed the three-phase induction motor drive, taking into account different schemes and using the proposed techniques.

In the final years of the past decade, limited literature was available on the dynamic stability of isolated three-phase induction generators [9,10]. These works are insufficient compared with the well-documented three-phase induction motor, as discussed above. The work in [9] dealt with the steady-state analysis of the three-phase isolated induction generator feeding an induction motor (IM) load using the predictor-corrector-type continuation method. Eigenvalue analysis was also used to examine the stability of the induction generator. On the other hand, the phase-plane plot, eigenvalue, and root-locus techniques were used to analyze the dynamic stability of the two parallel operated autonomous induction generators supplying an induction motor with long-shunt compensation in [10]. In [11–13], the stability of the three-phase synchronous machine was examined by using small signal analysis, Nyquist stability criteria, and the root-locus technique, respectively.

To the best of our knowledge, the stability analysis of the three-phase AC machine has been carried out

*Correspondence: kiransinghiitr@gmail.com

in detail in the aforementioned literature. Such analysis was not developed for multiphase AC machines until 2002. The stability issue using small-signal analysis of a multiphase machine was recognized first by Singh et al. [14] in 2003, followed by Duran et al. in 2008 [15] and Singh et al. in 2014 [16]. The authors in [14] analyzed the stability of a six-phase induction machine, considering the effect of common mutual leakage reactance between the two three-phase stator winding sets and supply harmonics. Conversely, [15] and [16] analyzed a five-phase motor with an injection of third harmonics and a six-phase synchronous generator connected to the utility grid, respectively. Such analysis contains no evidence for six-phase induction generators in isolated mode.

Small signal analysis with an eigenvalue approach focuses on a simple, stable, and successful operation under any balanced operating condition during small excursion behavior of a machine. Eigenvalue analysis is also employed to determine the critical operating conditions of the studied machine. In this paper, a linearized model of a six-phase isolated generator in d-q variables in a synchronously rotating reference frame is developed from the voltage equations of a multiphase induction machine [17]. In the present analysis, an eleventh-order linearized model for the SP-SEIG is developed for the dynamic stability analysis. The stability is investigated under perturbation of any one variable from the placement of the eigenvalues of the machine. In this linearized model, the effects of common mutual leakage inductance (L_{lm}) on two three-phase winding sets and cross-saturation coupling (L_{ldq}) between the d- and q-axis of the individual stator have not been considered in order to avoid the complexity of the solution. This analysis also presents the effect of magnetizing inductance during the process of self-excitation and finds that speed plays an important role, which is necessary for initiating and sustaining the self-excitation process in an isolated SP-SEIG for a given value of capacitance and load. Magnetizing inductance (L_m) also plays an important role in the dynamics of voltage build-up and stabilization of the SP-SEIG.

2. Fundamental modeling of SP-SEIG

2.1. Modeling of stator dynamics

An AC machine can have as many phases as coils per pole pair. Generally, all three-phase machines are designed with 60° phase belts, but sometimes these machines are also wound with 120° phase belts. A three-phase machine can be easily converted to six-phase by 'splitting' the 60° phase belts into two portions, each spanning 30°, without any additional cost. The detailed design of a six-phase machine was given in [17].

The equivalent circuit of the SP-SEIG is shown in = 1. The voltage and electromagnetic torque equations can be elaborated in the form of machine variables (the current is selected as an independent variable) for a six-phase induction generator in an arbitrary reference frame [18] by using Park's transformation, which converts the nonlinear differential equations with time-dependent inductance terms (three-phase axis model) into simplified equations with constant inductance terms (two-phase axis model):

$$V_{1q} = -r_1 i_{q1} + p\psi_{d1} + p\psi_{q1}; \tag{1}$$

$$V_{1d} = -r_1 i_{d1} - p\psi_{q1} + p\psi_{d1}; \tag{2}$$

$$V_{2q} = -r_2 i_{q2} + p\psi_{d2} + p\psi_{q2}; \tag{3}$$

$$V_{2d} = -r_2 i_{d2} - p\psi_{q2} + p\psi_{d2}; \tag{4}$$

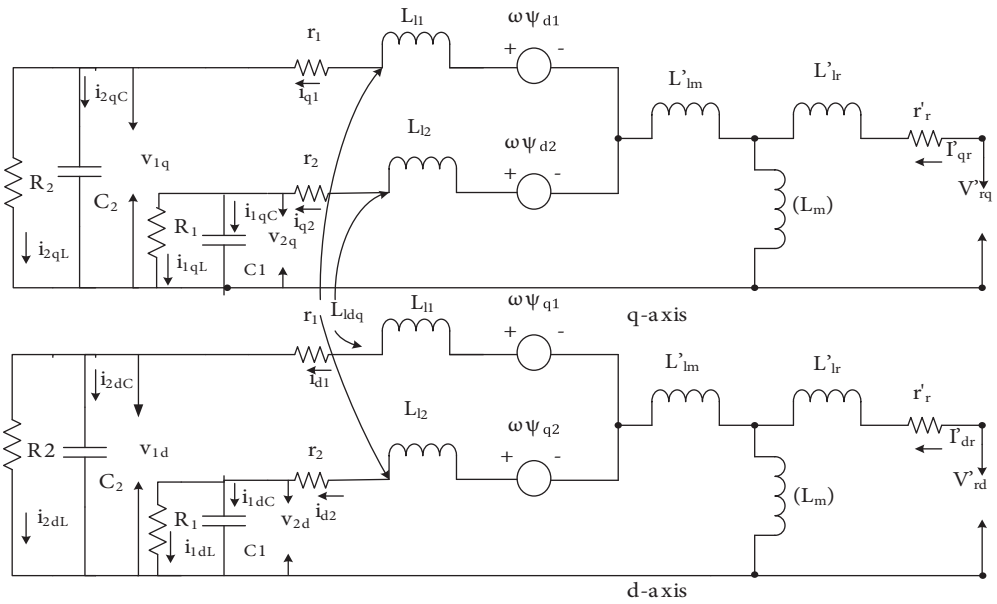

Figure 1. Equivalent circuit of SP-SEIG in dq axis.

$$V'_{rq}=r'_r i'_{qr}+(p-p_r)\psi'_{dr}+p\psi'_{qr}; \tag{5}$$

$$V'_{rd}=r'_r i'_{dr}-(p-p_r)\,\psi'_{qr}+p\psi'_{dr}; \tag{6}$$

$$\psi_{q1}=-L_{l1}i_{q1}+\psi_{qm};\psi_{d1}=-L_{l1}i_{d1}+\psi_{dm};\psi_{q2}=-L_{l2}i_{q2}+\psi_{qm}; \tag{7}$$

$$\psi_{d2}=-L_{l2}i_{d2}+\psi_{dm};\psi'_{qr}=-L'_{lr}i'_{qr}+\psi_{qm};\psi'_{dr}=-L'_{lr}i'_{dr}+\psi_{dm}; \tag{8}$$

where:

$$\psi_{dm}=L_{dm}i_{dm};\psi_{qm}=L_{qm}i_{qm};i_{dm}=-i_{d1}-i_{d2}+i'_{dr};i_{qm}=-i_{q1}-i_{q2}+i'_{qr}$$

Simplifying Eqs. (1)–(6) by using Eqs. (7) and (8), they can be rewritten as follows.

$$V_{1d}=-r_1 i_{d1}+p(L_{l1}+L_{dm})i_{q1}+pL_{qm}i_{q2}-pL_{qm}i'_{qr}-p(L_{l1}+L_{dm})i_{d1}-pL_{dm}i_{d2}+pL_{dm}i'_{dr} \tag{9}$$

$$V_{1q}=-r_1 i_{q1}-p(L_{l1}+L_{dm})i_{d1}-pL_{dm}i_{d2}+pL_{dm}i'_{dr}-p(L_{l1}+L_{qm})i_{q1}-pL_{qm}i_{q2}+pL_{qm}i'_{qr} \tag{10}$$

$$V_{2d}=-r_2 i_{d2}+p(L_{l2}+L_{qm})i_{q2}+pL_{qm}i_{q1}-pL_{qm}i'_{qr}-p(L_{l2}+L_{dm})i_{d2}-pL_{dm}i_{d1}+pL_{dm}i'_{dr} \tag{11}$$

$$V_{2q}=-r_2 i_{q2}-p(L_{l2}+L_{dm})i_{d2}-pL_{dm}i_{d1}+pL_{dm}i'_{dr}-p(L_{l2}+L_{qm})i_{q2}-pL_{qm}i_{q1}+pL_{qm}i'_{qr} \tag{12}$$

In the induction machine, rotor windings are short-circuited, and hence $V'_{rd}=V'_{rq}=0$.

$$0=r'_r i'_{qr}+(p-p_r)\,(L'_{lr}+L_{dm})i'_{dr}-(p-p_r)\,L_{dm}i_{d1}-(p-p_r)\,L_{dm}i_{d2}+p(L'_{lr}+L_{qm})i'_{qr}-pL_{qm}i_{q1}-pL_{qm}i_{q2} \tag{13}$$

$$0=r'_r i'_{dr}-(p-p_r)\,(L'_{lr}+L_{qm})i'_{qr}+(p-p_r)\,L_{qm}i_{q1}+(p-p_r)\,L_{qm}i_{q2}+p(L'_{lr}+L_{dm})i'_{dr}-pL_{dm}i_{d1}-pL_{dm}i_{d2} \tag{14}$$

For uniform air gap length, $L_{dm} = L_{qm} = L_m$, the equation for L_m was given in [17]:

$$L_m = 0.0002i_m^3 - 0.004i_m^2 + 0.019i_m + 0.1031, \tag{15}$$

$$i_m = \sqrt{[(-i_{d1} - i_{d2} + i'_{dr})^2 + (-i_{q1} - i_{q2} + i'_{qr})^2]}. \tag{16}$$

2.2. Modeling of shunt excitation capacitor bank and load

The mathematical modeling of both sets of the shunt excitation capacitor bank, connected in parallel with pure resistive loads, can be written in the ($dq0$) axis [18] as shown below.

$$pV_{1d} = (i_{1dc}/C_1) + pV_{1q} \tag{17}$$

$$pV_{1q} = (i_{1qc}/C_1) - pV_{1d} \tag{18}$$

$$pV_{2d} = (i_{2dc}/C_2) + pV_{2q} \tag{19}$$

$$pV_{2q} = (i_{2qc}/C_2) - pV_{2d} \tag{20}$$

According to Kirchhoff's current law, the current equations at the excitation shunt capacitor terminals respectively are given as:

$$i_{1dc} = i_{d1} - i_{1dL}; i_{1qc} = i_{q1} - i_{1qL}; i_{2dc} = i_{d2} - i_{2dL}; i_{2qc} = i_{q2} - i_{2qL}; \tag{21}$$

$$i_{1dc} = C_1 pV_{1d}; i_{1qc} = C_1 pV_{1q}; i_{2dc} = C_2 pV_{2d}; i_{2qc} = C_2 pV_{2q}. \tag{22}$$

If a pure resistive load is considered across the terminal of the generator, the load current equations can be given by:

$$i_{1dL} = V_{1d}/R_1; i_{1qL} = V_{1q}/R_1; i_{2dL} = V_{2d}/R_2; i_{2qL} = V_{2q}/R_2. \tag{23}$$

Hence, with pure resistive load, the q- and d-axis voltage equations can be modified as follows.

$$pV_{1d} = (i_{d1}/C_1) - (V_{1d}/R_1C_1) + pV_{1q} \tag{24}$$

$$pV_{1q} = (i_{q1}/C_1) - (V_{1q}/R_1C_1) - pV_{1d} \tag{25}$$

$$pV_{2d} = (i_{d2}/C_2) - (V_{2d}/R_2C_2) + pV_{2q} \tag{26}$$

$$pV_{2q} = (i_{q2}/C_2) - (V_{2q}/R_2C_2) - pV_{2d} \tag{27}$$

2.3. Modeling of torque and rotor dynamics

The electromagnetic torque and rotor speed of the SP-SEIG can be expressed in terms of selected state-space variables as:

$$Te = (3/2)(P/2)(Lm/Lr)[(i_{q1} + i_{q2})\Psi'_{dr} - (i_{d1} + i_{d2})\Psi'_{qr}], \tag{28}$$

$$\omega_r = (1/p)(P/2)(1/J)(Te - Tm), \tag{29}$$

where T_e is electromagnetic torque, T_m... is mechanical input torque, and $L_r = L'_{lr} + L_m$.

After combining Eqs. (9)–(14) and Eqs. (24)–(29), it is convenient to write the system equations in a synchronously rotating reference frame by setting $\omega = \omega_e$ and rewrite them in matrix form as given in Eq. (30). All other symbols used are explained in Table 1.

Table 1. Nomenclature.

Symbols	Description	Symbols	Description
V_{1d}, V_{1q}	d-q axis voltage of winding set I	ω_e	Synchronously rotating reference frame speed
V_{2d}, V_{2q}	d-q axis voltage of winding set II	θ_r	Electrical angular displacement of the rotor
V'_{rd}, V'_{rq}	d-q axis rotor voltage referred to stator	r_1, r_2	Stator resistance per phase of stator sets I and II
$\psi_{d1}\psi_{q1}$	d -q axis flux linkage per second of winding set I	r'_r	Rotor resistance per phase referred to stator
ψ_{d2}, ψ_{q2}	d -q axis flux linkage per second of winding set II	L_{l1}, L_{l2}	Stator leakage inductance per phase of stator sets I and II
ψ'_{dr}, ψ'_{qr}	d-q axis rotor flux linkage per second referred to stator	L'_{lr}	Rotor leakage inductance per phase referred to stator
i_{d1}, i_{q1}	d-q axis current of winding set I	L_m	Steady-state saturated magnetizing inductance
i_{d2}, i_{q2}	d-q axis current of winding set II	i_{1d_c}, i_{1qc}	d-q axis current through shunt capacitor across winding set I
i'_{dr}, i'_{qr}	d-q axis rotor current referred to stator	i_{2dc}, i_{2qc}	d-q axis current through shunt capacitor across winding set II
P	Number of poles	i_{1dL}, i_{1qL}	d-q axis current along resistive load across winding set I
J	Moment of inertia	i_{2dL}, i_{2qL}	d-q axis current along resistive load across winding set II
ω	Speed of the reference frame	C_1, C_2	Shunt capacitor per phase along stator sets I and II
ω_r	Rotor speed	R_1, R_2	Resistive load per phase along stator sets I and II

3. Development of linearized SP-SEIG model

The behavior of induction machines is nonlinear, so there is a need for linearization of these nonlinear equations and for rewriting them in state variable form for further analysis. The procedure involved in the linearization of nonlinear differential equations of the SP-SEIG has included the assumptions for small displacement. First, the product terms of two or more deviations must be neglected. Second, flux levels have little variation for keeping the inductance terms constant. In the process of linearization, initially each variable is replaced by its value, and then both the assumptions are applied for simplifying the linearized differential equations. In this way, small-displacement linear equations are developed from a fixed operating point. The linear differential equations of the SP-SEIG are given in Eq. (31). The linearized machine equations are conveniently derived from the voltage equations with currents as state variables under steady-state balanced conditions. This selection is generally determined by a particular application.

The resulting set of differential equations are linear with regard to small disturbances.

$$\begin{bmatrix} 0 \\ 0 \\ 0 \\ 0 \\ V'_{rd} \\ V'_{rq} \\ 0 \\ 0 \\ 0 \\ 0 \\ T_m \end{bmatrix} = \begin{bmatrix} -r_1-p(L_{l1}+L_m) & \omega_e(L_{l1}+L_m) & -pL_m & \omega_eL_m & pL_m & -\omega_eL_m & -1 & 0 & 0 & 0 & 0 \\ -\omega_e(L_{l1}+L_m) & -r_1-p(L_{l1}+L_m) & -\omega_eL_m & -pL_m & \omega_eL_m & pL_m & 0 & -1 & 0 & 0 & 0 \\ -pL_m & \omega_eL_m & -r_2-p(L_{l2}+L_m) & -\omega_e(L_{l2}+L_m) & pL_m & -\omega_eL_m & 0 & 0 & -1 & 0 & 0 \\ -\omega_eL_m & -pL_m & -\omega_e(L_{l2}+L_m) & -r_2-p(L_{l2}+L_m) & \omega_eL_m & pL_m & 0 & 0 & 0 & -1 & 0 \\ -pLm & (\omega_e-\omega_r)L_m & -pL_m & (\omega_e-\omega_r)L_m & r'_r+p(L'_{lr}+L_m) & -(\omega_e-\omega_r)(L'_{lr}+L_m) & 0 & 0 & 0 & 0 & 0 \\ -(\omega_e-\omega_r)L_m & -pL_m & -(\omega_e-\omega_r)L_m & -pL_m & (\omega_e-\omega_r)(L'_{lr}+L_m) & r'_r+p(L'_{lr}+L_m) & 0 & 0 & 0 & 0 & 0 \\ -1/C_1 & 0 & 0 & 0 & 0 & 0 & (-p-1/R_1C_1) & \omega_e & 0 & 0 & 0 \\ 0 & -1/C_1 & 0 & 0 & 0 & 0 & -\omega_e & (-p-1/R_1C_1) & 0 & 0 & 0 \\ 0 & 0 & -1/C_2 & 0 & 0 & 0 & 0 & 0 & (-p-1/R_2C_2) & \omega_e & 0 \\ 0 & 0 & 0 & -1/C_2 & 0 & 0 & 0 & 0 & -\omega_e & (-p-1/R_2C_2) & 0 \\ -k_2L_mi'_{qr} & k_1L_mi'_{dr} & -k_2L_mi'_{qr} & k_1L_mi'_{dr} & L'_{lr}(i_{q1}+i_{q2}) & -L'_{lr}(i_{d1}+i_{d2}) & 0 & 0 & 0 & 0 & -p(2J/P) \end{bmatrix} \begin{bmatrix} i_{d1} \\ i_{q1} \\ i_{d2} \\ i_{q2} \\ i'_{dr} \\ i'_{qr} \\ V_{1d} \\ V_{1q} \\ V_{2d} \\ V_{2q} \\ \omega_r \end{bmatrix} \tag{30}$$

$$\begin{bmatrix} 0 \\ 0 \\ 0 \\ 0 \\ V'_{rd} \\ V'_{rq} \\ 0 \\ 0 \\ 0 \\ 0 \\ T_m \end{bmatrix} = \begin{bmatrix} -r_1-p(L_{l1}+L_m) & \omega_e(L_{l1}+L_m) & -pL_m & \omega_eL_m & pL_m & -\omega_eL_m & -1 & 0 & 0 & 0 & 0 \\ -\omega_e(L_{l1}+L_m) & -r_1-p(L_{l1}+L_m) & -\omega_eL_m & -pL_m & \omega_eL_m & pL_m & 0 & -1 & 0 & 0 & 0 \\ -pL_m & \omega_eL_m & -r_2-p(L_{l2}+L_m) & -\omega_e(L_{l2}+L_m) & pL_m & -\omega_eL_m & 0 & 0 & -1 & 0 & 0 \\ -\omega_eL_m & -pL_m & -\omega_e(L_{l2}+L_m) & -r_2-p(L_{l2}+L_m) & \omega_eL_m & pL_m & 0 & 0 & 0 & -1 & 0 \\ -pLm & (\omega_e-\omega_r)L_m & -pL_m & (\omega_e-\omega_r)L_m & r'_r+p(L'_{lr}+L_m) & -(\omega_e-\omega_r)(L'_{lr}+L_m) & 0 & 0 & 0 & 0 & -Lm(iq10+iq20)+(L'lr+Lm)i'qr0 \\ -(\omega_e-\omega_r)L_m & -pL_m & -(\omega_e-\omega_r)L_m & -pL_m & (\omega_e-\omega_r)(L'_{lr}+L_m) & r'_r+p(L'_{lr}+L_m) & 0 & 0 & 0 & 0 & Lm(id10+id20)+(L'lr+Lm)i'dr0 \\ -1/C_1 & 0 & 0 & 0 & 0 & 0 & (-p-1/R_1C_1) & \omega_e & 0 & 0 & 0 \\ 0 & -1/C_1 & 0 & 0 & 0 & 0 & -\omega_e & (-p-1/R_1C_1) & 0 & 0 & 0 \\ 0 & 0 & -1/C_2 & 0 & 0 & 0 & 0 & 0 & (-p-1/R_2C_2) & \omega_e & 0 \\ 0 & 0 & 0 & -1/C_2 & 0 & 0 & 0 & 0 & -\omega_e & (-p-1/R_2C_2) & 0 \\ -k_2L_mi'_{qr0} & k_1L_mi'_{dr0} & -k_2L_mi'_{qr0} & k_1L_mi'_{dr0} & (L'lr(iq10+iq20)) & (-L'lr(id10+id20)) & 0 & 0 & 0 & 0 & -p(2J/P) \end{bmatrix} \begin{bmatrix} i_{d1} \\ i_{q1} \\ i_{d2} \\ i_{q2} \\ i'_{dr} \\ i'_{qr} \\ V_{1d} \\ V_{1q} \\ V_{2d} \\ V_{2q} \\ \omega_r \end{bmatrix} \tag{31}$$

where,

$$p_1 = (((3P)/4)\,(Lm/(Lm+L'lr)))$$
$$p_2 = (((3P)/4)\,(Lm/(Lm+L'lr)))$$

Eq. (32) in the state space form is written as:

$$Apx = Bx + u \tag{32}$$

where $x = \begin{bmatrix} i_{d1} & i_{q1} & i_{d2} & i_{q2} & i'_{dr} & i'_{qr} & V_{1d} & V_{1q} & V_{2d} & V_{2q} & \omega_r \end{bmatrix}^T$,
$u = \begin{bmatrix} 0 & 0 & 0 & 0 & V'_{rd} & V'_{rq} & 0 & 0 & 0 & 0 & T_m \end{bmatrix}^T$, and A and B are given by Eqs. (33) and (34).

$$\mathbf{A} = \begin{bmatrix} -(Ll1+Lm) & 0 & -Lm & 0 & Lm & 0 & 0\,0\,0\,0 & 0 \\ 0 & -(Ll1+Lm) & 0 & -Lm & 0 & Lm & 0\,0\,0\,0 & 0 \\ -Lm & 0 & -(Ll2+Lm) & 0 & Lm & 0 & 0\,0\,0\,0 & 0 \\ 0 & -Lm & 0 & -(Ll2+Lm) & 0 & Lm & 0\,0\,0\,0 & 0 \\ -Lm & 0 & -Lm & 0 & (L'lr+Lm) & 0 & 0\,0\,0\,0 & 0 \\ 0 & -Lm & 0 & -Lm & 0 & (L'lr+Lm) & 0\,0\,0\,0 & 0 \\ 0 & 0 & 0 & 0 & 0 & 0 & 1\,0\,0\,0 & 0 \\ 0 & 0 & 0 & 0 & 0 & 0 & 0\,1\,0\,0 & 0 \\ 0 & 0 & 0 & 0 & 0 & 0 & 0\,0\,1\,0 & 0 \\ 0 & 0 & 0 & 0 & 0 & 0 & 0\,0\,0\,1 & 0 \\ 0 & 0 & 0 & 0 & 0 & 0 & 0\,0\,0\,0 & -(2J/P) \end{bmatrix} \tag{33}$$

$$B = \begin{bmatrix}
-r1 & \omega e(Ll1+Lm) & 0 & \omega eLm & 0 & -\omega eLm & -1 & 0 & 0 & 0 & 0 \\
-\omega e(Ll1+Lm) & -r1 & -\omega eLm & 0 & \omega eLm & 0 & 0 & -1 & 0 & 0 & 0 \\
0 & \omega eLm & -r2 & -\omega e(Ll2+Lm) & 0 & -\omega eLm & 0 & 0 & -1 & 0 & 0 \\
-\omega eLm & 0 & -\omega e(Ll2+Lm) & -r2 & \omega eLm & 0 & 0 & 0 & 0 & -1 & 0 \\
0 & (\omega e-\omega r)Lm & 0 & (\omega e-\omega r)Lm & r'r & -(\omega e-\omega r)(L'lr+Lm) & 0 & 0 & 0 & 0 & -Lm(iq10+iq20)+(L'lr+Lm)i'qr0 \\
-(\omega e-\omega r)Lm & 0 & -(\omega e-\omega r)Lm & 0 & (\omega e-\omega r)(L'lr+Lm) & r'r & 0 & 0 & 0 & 0 & Lm(id10+id20)+(L'lr+Lm)i'dr0 \\
-1/C1 & 0 & 0 & 0 & 0 & 0 & -(1/R1C1) & \omega e & 0 & 0 & 0 \\
0 & -1/C1 & 0 & 0 & 0 & 0 & -\omega e & -(1/R1C1) & 0 & 0 & 0 \\
0 & 0 & -1/C2 & 0 & 0 & 0 & 0 & 0 & -(1/R2C2) & \omega e & 0 \\
0 & 0 & 0 & -1/C2 & 0 & 0 & 0 & 0 & -\omega e & -(1/R2C2) & 0 \\
(-k_2Lmi'qr0) & (k_1Lmi'dr0) & (-k_2Lmi'qr0) & (k_1Lmi'dr0) & (L'lr(iq10+iq20)) & (-L'lr(id10+id20)) & 0 & 0 & 0 & 0 & 0
\end{bmatrix} \quad (34)$$

and the subscript '0' denotes steady-state values.

It is also suitable to indicate Eq. (32) in the elementary form of a linear differential equation (state equation). This standard state equation can be written as:

$$px = A^{-1}Bx + A^{-1}u \tag{35}$$

where

$$E = A^{-1}B \tag{36}$$

$$F = A^{-1} \tag{37}$$

The linear differential equations written in standard or state variable form in Eq. (35) can be rewritten as:

$$px = Ex + Fu \tag{38}$$

where u is the input vector, and if it is equal to zero, the solution of linear differential Eq. (35) can be given by Eq. (39). The characteristic equation of A is determined by Eq. (40) from [18]:

$$x = Ke^{At} \tag{39}$$

and

$$\det(A - \zeta I) = 0 \tag{40}$$

where roots ζ of Eq. (40) are referred to as eigenvalues, characteristic roots, or latent roots, and I is an identity matrix.

4. Eigenvalue analysis of small signal

Eigenvalues allow a direct and effective approach for stability analysis of the SP-SEIG at any small displacement. These are either real or complex values obtained from the characteristic equation of the studied system. Real values correlate with the nonoscillatory mode of the state variables. Positive and negative real values indicate a periodic instability and a decaying mode, respectively. However, when they are complex, they occur as a pair of complex-conjugate eigenvalues that signifies a mode of oscillation of the state variables. The real part of the complex-conjugate eigenvalue corresponds to damping, whereas the imaginary part corresponds to the

frequency of oscillations. Real parts may be either positive or negative. Positive values indicate an exponential increase with time (an unstable condition), and negative values indicate an exponential decrease with time (a stable condition). Basic linear system theory can be used to calculate the eigenvalues [1,3,4,18–22].

The eigenvalues of the SP-SEIG can be obtained by using the standard eigenvalue computer routine. To calculate the roots of matrix [E] given by Eq. (40), i.e. the eigenvalues of the SP-SEIG, a computer program has been developed from Eq. (39). The eleven state variables contribute to a set of eleven eigenvalues. The sets of eigenvalues are given in Table 2 for small displacement at three different equilibrium points (different rotor speeds). It is also important to consider the saturation effect in the SP-SEIG in order to express the nonlinear nature of magnetizing reactance. The nonlinear characteristic relating magnetizing inductance (L_m) to magnetizing current (I_m) is determined by standard experimental tests. During self-excitation, variation in the value of magnetizing inductance due to saturation is the main factor in dynamics of voltage build and stabilization. The transient response of unstable voltage points of the SP-SEIG is shown in Figure 2a. No load voltage is shown in Figures 2b and 2c. The effect of magnetizing inductance in self-excitation with speed is shown in Figure 2d when both the winding sets are connected to 38.5 μF. The experimental setup (Figure 3) is arranged in an electrical lab of the Alternate Hydro Energy Center, Indian Institute of Technology Roorkee, Roorkee, Uttarakhand, India. The machine parameters (per phase) are also given in Table 3. At stall, one of the eigenvalues of the studied system has zero real part, and hence the self-excitation of the studied system will be initiated. When the speed increases from stall to a rated (no load) speed from their respective columns 1 to 2 (3), one of the eigenvalues has a positive real part, as given in Table 2, and tends to sustainable self-excitation. In the following ways, variations of eigenvalues have been determined to analyze the study of stability by varying the minimum shunt capacitance, (varying machine parameters, and varying system loading.

4.1. Effect of shunt capacitance required for self-excitation

The minimum capacitance required for self-excitation can be determined by any scheme as given in [22,23]. As in [22], the value of the minimum capacitance depends on the eigenvalues of system matrix A, whereas in [23], it

Table 2. Eigenvalues (rad/s) of the studied system under no load.

Eigenvalues (rad/s)	Significance of eigenvalues	Stall N_r= 0 rpm id1 = 0 id2 = id1 iq1 = 0 iq2 = iq1 idr = 0 iqr = idr	Synchronous speed N_r= 1137.34 rpm id1 = 3.9514 id2 = id1 iq1 = –3.9514 iq2 = iq1 idr = 0.4903 iqr = idr	Rated speed N_r= 1132.691 rpm id1 = 4.012 id2 = id1 iq1 = –4.012 iq2 = iq1 idr = 0.4950 iqr = idr
I	Stator eigenvalues	–17.514 ± 1162.647i	–17.531 ± 1163.055i	–17.668 ± 1163.107i
II		–166.646 ± 902.778i	–154.239 ± 899.185i	–154.397 ± 900.421i
III	Rotor eigenvalue	–11.557 ± 651.911i	–43.835 ± 633.862i	–43.512 ± 634.491i
IV	Capacitor eigenvalues	–23.199 ± 321.009i	–76.018 ± 317.838i	–77.0425 ± 323.389i
V		–187.058 ± 295.855i	–119.147 ± 38.866i	–118.449 ± 37.272i
VI	Real eigenvalue	0.000 + 0.000i	9.590 + 0.000i	9.925 + 0.000i

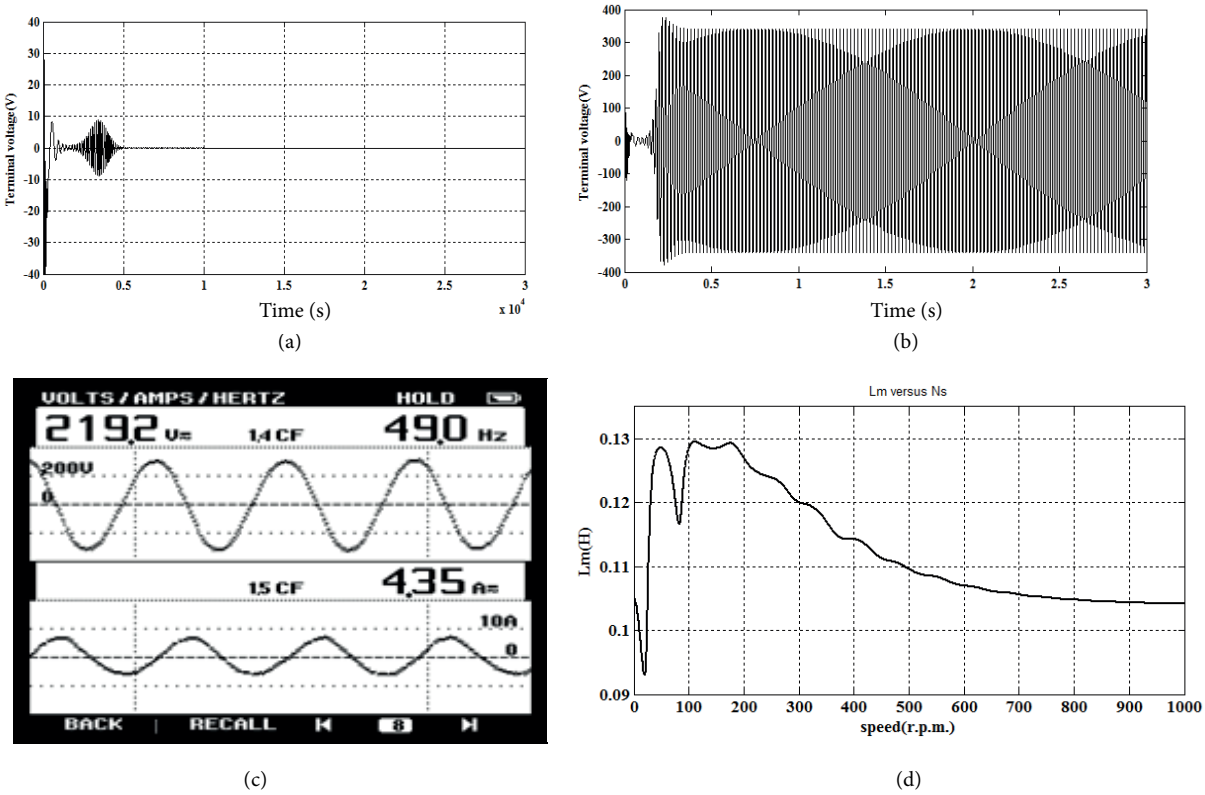

Figure 2. Transient response of: (a) unstable points from column 1 of Tables 4 and 5, (b) simulated no-load terminal voltage, (c) experimental no-load terminal voltage, and (d) relation between magnetizing inductance (L_m) and no-load machine speed.

Figure 3. Laboratory set-up with stator winding arrangement.

depends on the optimization constraints so as to achieve better performance. A minimum value of capacitance (38.5 μF) is determined by the magnitude and nature of the eigenvalue. When one of the eigenvalues has zero real part, as illustrated in Table 2, the self-excitation phenomenon has been initiated. In Tables 4 and 5, efforts are made to examine the magnitude and nature of all eigenvalues w.r.t. the minimum value of capacitance and rated frequency. This effort shows the effects of the other values of capacitance moving from the first to last column of Tables 4 and 5. There are abrupt variations in the imaginary parts and/or the rated frequency of

stator eigenvalues. These variations of eigenvalues are tabulated in Tables 4 and 5 at no-load on synchronous speed and rated speed, respectively. In Tables 4 and 5, when the movement is from column 1 to 3, the frequency of stator eigenvalue IV starts increasing. This corresponds to unstable operation, as shown already in Figure 2a.

Table 3. Parameters of a 1.1-kW, 36-slot, 6-pole, 6-phase, 415-V, 2.9-A, 50-Hz, and 960-RPM squirrel cage induction machine.

Measured parameters	Value/phase	Measured parameters	Value/phase
Stator resistance r_1, r_2	4.12 Ω	Rotor leakage inductance L_{lr}	43.3 mH
Stator leakage inductance L_{l1}, L_{l2}	21.6 mH	Magnetizing inductance L_m	234.6 mH
Rotor resistance r_r	8.79 Ω	Self-excitation capacitance C_1, C_2	38.5 μF

Table 4. Comparison of eigenvalues from C_{min} to higher C at synchronous speed.

id1 = 3.9514 id2 = id1 iq1 = –3.9514 iq2 = iq1 idr = 0.4903 iqr = idr Nr = 1137.34 C_{min}= 38.5 μF	id1 = 3.313 id2 = id1 iq1 = –3.313 iq2 = iq1 idr = 0.5884 iqr = idr Nr = 812.6 C_1= C_2= 78.5 μF	id1 = 2.883 id2 = id1 iq1 = –2.883 iq2 = iq1 idr = 0.6082 iqr = idr Nr = 650 C_1= C_2= 118.5 μF
–17.668 ± 1163.109i	–13.691 ± 848.215i	–12.172 ± 715.445i
–154.343 ± 900.412i	–614.831 + 0.000i	–747.475 + 0.000i
	281.735 + 0.000i	408.278 + 0.000i
–43.733 ± 634.411i	–132.102 ± 605.217i	–122.182 ± 503.961i
–77.094 ± 323.471i	–26.153 ± 496.442i	–19.460 ± 442.395i
–118.033 ± 39.439i	–73.278 ± 59.517i	–85.917 ± 119.507i
9.532 + 0.000i	11.334 + 0.000i	6.447 + 0.000i

4.2. Effect of machine parameters

The variation of eigenvalues with machine parameters has also been determined. These parameters are stator resistance, rotor resistance, stator leakage inductance, rotor leakage inductance, magnetizing inductance, and inertia constant. The most critical parameter is the variation of magnetizing inductance (L_m) in the dynamics of voltage build-up and stabilization of the SP-SEIG. With the change in magnetizing inductance, all eigenvalues are slightly affected, as shown in Figure 4.

4.3. Effect of system loading

The effects of resistive loading, for a fixed excitation/fixed reactive power, on the rotor eigenvalues are depicted in Table 6 for rated speed and synchronous speed. According to the real eigenvalues presented in Table 6, the studied system is moving from an unstable point (column 1) to a stable point (columns 2 to 3). This means that machine operation tends to be more stable. When real eigenvalues are negative, self-excitation cannot be initiated and/or cannot be sustained, as shown in Figure 2a. On the contrary, when real eigenvalues are positive, self-excitation will be initiated and sustained, as shown in Figures 2b and 2c. In Figure 2a, voltage generation is initiated, but after a very short time period it dies out. Figures 2b and 2c depict the analytical and experimental waveforms of terminal voltage and the current of a system at no-load speed of 1000 RPM,

Table 5. Comparison of eigenvalues from C_{min} to higher C at rated speed.

id1 = 4.012 id2 = id1 iq1 = –4.012 iq2 = iq1 idr = 0.4950 iqr = idr Nr = 1132.69 C_{min}= 38.5 μF	id1 = 3.394 id2 = id1 iq1 = –3.394 iq2 = iq1 idr = 0.6059 iqr = idr Nr = 815.686 C_1= C_2= 78.5 μF	id1 = 2.97 id2 = id1 iq1 = –2.97 iq2 = iq1 idr = 0.495 iqr = idr Nr = 657.2 C_1= C_2= 118.5 μF
–17.668 ± 1163.107i	–13.692 ± 848.216i	–12.172 ± 715.455i
–154.397 ± 900.421i	–614.811 + 0.000i	–747.328 + 0.000i
	281.727 + 0.000i	408.512 + 0.000i
–43.512 ± 634.491i	–132.065 ± 605.217i	–121.898 ± 503.966
–77.042 ± 323.389i	–26.171 ± 496.406i	–19.613 ± 442.336i
–118.449 ± 37.272i	–73.611 ± 58.481i	–86.202 ± 116.908i
9.925 + 0.000i	11.952 + 0.000i	6.377 + 0.000i

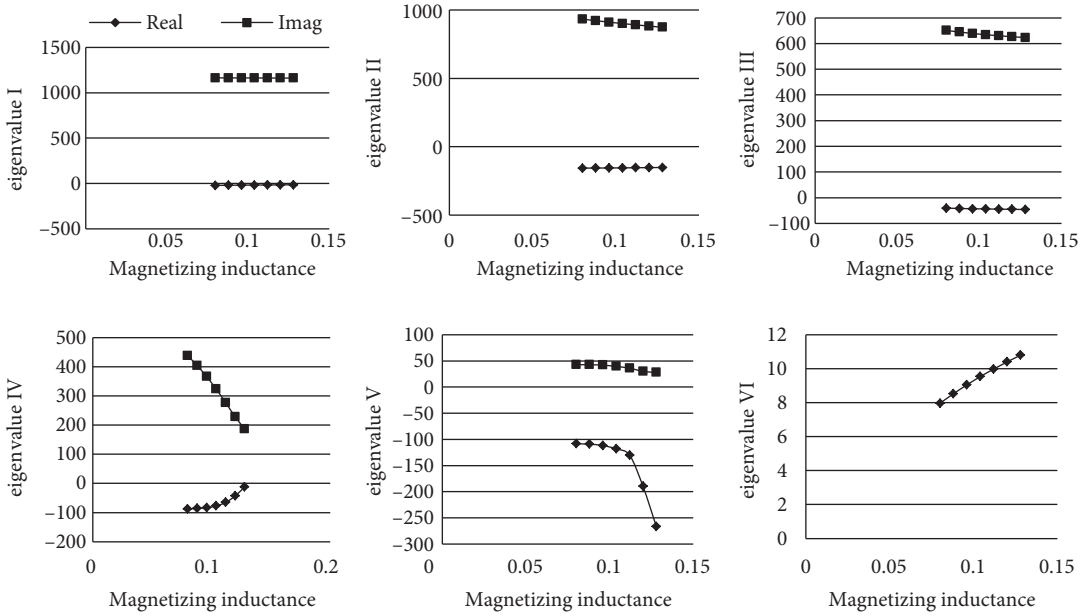

Figure 4. Eigenvalue variations with small perturbation in magnetizing inductance.

respectively. Once the voltage has been established, the stability around the equilibrium point can be evaluated when the studied system is referred to a reference rotating frame. Table 2 shows the system eigenvalues for three different equilibrium points with no load. Table 6 shows the system eigenvalues under six different equilibrium points for the system with load.

5. Conclusion

Stability studies of the SP-SEIG are developed by using a simple method based on eigenvalue analysis. Eigenvalues play an important role in the selection of minimum capacitance required for self-excitation and the condition at which excitation will be initiated and sustained. When one of the eigenvalues has zero real part, it gives the minimum capacitance value to initiate the self-excitation of the machine, and when one of the eigenvalues has a positive real part, self-excitation will be initiated and sustained. From the analysis, it is demonstrated that

Table 6. Eigenvalues (rad/s) under resistive loading conditions.

At rated speed			At synchronous speed		
id1 = 1.9739 id2 = id1 iq1 = 1.9742 iq2 = iq1 idr = 1.3455 iqr = idr N_r= 1093.73 rpm	id1 = 3.0878 id2 = id1 iq1 = 3.0878 iq2 = iq1 idr = 0.9445 iqr = idr N_r= 1068 rpm	id1 = 5.6742 id2 = id1 iq1 = 5.6742 iq2 = iq1 idr = 0.7000 iqr = idr N_r= 1132.69 rpm	id1 = 1.93 id2 = id1 iq1 = 1.93 iq2 = iq1 idr = 1.32 iqr = idr Nr = 1093.1968	id1 = 3 id2 = id1 iq1 = 3 iq2 = iq1 idr = 0.9163 iqr = idr Nr = 1062	id1 = 5.674 id2 = id1 iq1 = 5.674 iq2 = iq1 idr = 0.7 iqr = idr Nr = 1132.691
–17.669 ± 1163.102i	–17.668 ± 1163.093i	–17.668 ± 1163.107i	–17.669 ± 1163.102i	–17.668 ± 1163.091i	–17.531 ± 1163.055i
–154.528 ± 900.499i	–154.794 ± 900.532i	–154.397 ± 900.421i	–154.526 ± 900.497i	–154.839 ± 900.539i	–154.239 ± 899.185i
–43.087 ± 635.383i	–42.027 ± 635.707i	–43.512 ± 634.491i	–43.101 ± 635.386i	–41.864 ± 635.804i	–43.835 ± 633.862i
–77.284 ± 323.235i	–76.945 ± 322.808i	–77.042 ± 323.389i	–77.276 ± 323.243i	–76.898 ± 322.737i	–76.018 ± 317.838i
–112.937 ± 22.579i	–126.399 + 0.000i	–118.449 ± 37.272i	–112.952 ± 22.348i	–130.723 + 0.000i	–119.147 ± 38.866i
	–104.951 + 0.000i			–100.913 + 0.000i	
–1.200 + 0.000i	2.010 + 0.000i	9.925 + 0.000i	–1.162 + 0.000i	1.964 + 0.000i	9.590 + 0.000i

all the eigenvalues are affected by the change in magnetizing inductance (L_m), and this shows that the most critical parameter is a small perturbation in magnetizing inductance (L_m) in the dynamics of the SP-SEIG.

References

[1] Rogers GJ. Linearized analysis of induction-motor transients. P I Electr Eng 1965; 112: 1917-1926.

[2] Fallside FI, Wortley AT. Steady-state oscillation and stabilization of variable frequency Inverter fed induction motor drives. IEE Proc 1969; 116: 991-999.

[3] Lipo TA, Krause PC. Stability analysis of a rectifier-inverter induction motor drive. IEEE T Power Ap Syst 1969; 88: 55-66.

[4] Nelson RH, Lipo TA, Krause PC. Stability analysis of a symmetrical induction machine. IEEE T Power Ap Syst 1969; 88: 1710-1717.

[5] Cornell EP, Lipo TA. Modeling and design of controlled current induction motor drive systems. IEEE T Power Ap Syst 1977; 13: 321-330.

[6] Macdonald ML, Sen PC. Control loop study of induction motor drives using DQ model. IEEE T Ind El Con In 1979; 26: 237-243.

[7] Tan OT, Richards GG. Decoupled boundary layer model of induction machines. IEE Proc 1986; 133: 255-262.

[8] Ahmed MM, Tanfig JA, Goodman CJ, Lockwood M. Electrical instability in a voltage source inverter fed induction motor drive. IEE Proc 1986; 133: 299-307.

[9] Kuo SC, Wang L. Steady-state performance of a self-excited induction generator feeding an induction motor. Electric Pow Compo Sys 2002; 30: 581-593.

[10] Kuo SC, Wang L. Analysis of parallel-operated self-excited induction generators feeding an induction motor load with a long-shunt connection. Electric Pow Compo Sys 2004; 32: 1043-1060.

[11] Lipo TA, Krause PC. Stability analysis of a reluctance-synchronous machine. IEEE T Power Ap Syst 1967; 86: 825-834.

[12] Lipo TA, Krause PC. Stability analysis for variable frequency operation of synchronous machines. IEEE T Power Ap Syst 1968; 87: 227-234.

[13] Stapleton CA. Root-locus study of synchronous-machine regulation. IEE Proc 1964; 111: 761-768.

[14] Singh GK, Pant V, Singh YP. Stability analysis of a multiphase (six-phase) induction machine. Comput Electr Eng 2003; 29: 727-756.

[15] Duran MJ, Salas F, Arahal MR. Bifurcation analysis of five-phase induction motor drives with third harmonic injection. IEEE T Ind Electron 2008; 55: 2006-2014.

[16] Singh GK, Singh D. Small signal stability analysis of six-phase synchronous generator. Prz Elektrotechnicz 2013; 89: 76-82.

[17] Singh GK. Modelling and experimental analysis of a self-excited six-phase induction generator for stand-alone renewable energy generation. Renew Energ 2008; 33: 1605-1621.

[18] Krause PC. Analysis of Electric Machinery. New York, NY, USA: McGraw-Hill, 1986.

[19] Rangasamy S, Manickam P. Stability analysis of multimachine thermal power systems using the nature-inspired modified cuckoo search algorithm. Turk J Elec Eng & Comp Sci 2014; 22 : 1099-1115.

[20] Li W, Ching-Huei L. Dynamic analyses of parallel operated self-excited induction generators feeding an induction motor load. IEEE T Energy Conver 1999; 14: 479-485.

[21] Singh GK, Kumar AS, Saini RP. Selection of capacitance for self-excited six-phase induction generator for stand-alone renewable energy generation. Int J Energ 2010; 35: 3273-3283.